The NDC80 complex proteins Nuf2 and Hec1 make distinct contributions to kinetochore–microtubule attachment in mitosis

Lynsie J.R. Sundin, Geoffrey J. Guimaraes, and Jennifer G. DeLuca
Department of Biochemistry and Molecular Biology, Colorado State University, Fort Collins, CO 80523

ABSTRACT **Successful mitosis requires that kinetochores stably attach to the plus ends of spindle microtubules. Central to generating these attachments is the NDC80 complex, made of the four proteins Spc24, Spc25, Nuf2, and Hec1/Ndc80. Structural studies have revealed that portions of both Hec1 and Nuf2 N termini fold into calponin homology (CH) domains, which are known to mediate microtubule binding in certain proteins. Hec1 also contains a basic, positively charged stretch of amino acids that precedes its CH domain, referred to as the "tail." Here, using a gene silence and rescue approach in HeLa cells, we show that the CH domain of Hec1, the CH domain of Nuf2, and the Hec1 tail each contributes to kinetochore–microtubule attachment in distinct ways. The most severe defects in kinetochore–microtubule attachment were observed in cells rescued with a Hec1 CH domain mutant, followed by those rescued with a Hec1 tail domain mutant. Cells rescued with Nuf2 CH domain mutants, however, generated stable kinetochore–microtubule attachments but failed to generate wild-type interkinetochore tension and failed to enter anaphase in a timely manner. These data suggest that the CH and tail domains of Hec1 generate essential contacts between kinetochores and microtubules in cells, whereas the Nuf2 CH domain does not.**

Monitoring Editor
David G. Drubin
University of California, Berkeley

Received: Aug 5, 2010
Revised: Jan 3, 2011
Accepted: Jan 13, 2011

INTRODUCTION

At the onset of mitosis in vertebrate cells, the stable interphase microtubule network is converted into a bipolar spindle made up of short, dynamic microtubules. An essential function of these spindle microtubules is to capture mitotic chromosomes by attaching to a large protein structure, called the kinetochore, built at sites of centromeric heterochromatin. In many cases, the initial attachment between microtubules and kinetochores is along the length of a microtubule, and these lateral attachments must eventually be replaced by end-on attachments, where the plus ends of spindle microtubules are embedded in the kinetochore. When both sister kinetochores of a mitotic chromosome are attached in this manner, forces can be generated for directed chromosome movement and to silence the spindle assembly checkpoint.

The formation of stable, end-on kinetochore–microtubule connections depends on the kinetochore-associated NDC80 complex (Wigge and Kilmartin, 2001; DeLuca *et al.*, 2002; Martin-Lluesma *et al.*, 2002; McCleland *et al.*, 2004), which is a member of the conserved KMN network, containing also KNL1 and the Mis12 complex (Cheeseman *et al.*, 2006). The NDC80 complex is a long, dumbbell-shaped hetero-tetramer built from the individual proteins Spc24, Spc25, Nuf2, and Hec1 (also referred to as Ndc80). The C termini of Spc24 and Spc25 anchor the complex into the kinetochore, whereas N-terminal domains of Nuf2 and Hec1 reside exterior to Spc24 and Spc25, poised to interact with the plus ends of spindle microtubules (DeLuca *et al.*, 2006; Wan *et al.*, 2009). Both KNL1 and the NDC80 complex are able to bind microtubules in vitro; however, depletion of KNL1 from cultured cells results in less severe kinetochore–microtubule attachment defects than does depletion of NDC80 complex components (Cheeseman *et al.*, 2008). This has led to the idea that the NDC80 complex, aided by other factors including KNL1, serves as the primary contact between kinetochores and microtubules in cells.

Structural studies of the N terminus of Hec1 (Wei *et al.*, 2007), and of a modified NDC80 complex (NDC80^{Bonsai}) truncated of

This article was published online ahead of print in MBoC in Press (http://www.molbiolcell.org/cgi/doi/10.1091/mbc.E10-08-0671) on January 26, 2011.

Address correspondence to: Jennifer G. DeLuca: (jdeluca@colostate.edu).

Abbreviations used: ACA, anti-centromere antibody; BDS, boiled donkey serum; CH, calponin homology; DAPI, 4′-6-diamidino-2-phenylindole; DIC, differential interference contrast; FBS, fetal bovine serum; GFP, green fluorescent protein; SD, standard deviation; siRNA, small interfering RNA; WT, wild type.

© 2011 Sundin *et al.* This article is distributed by The American Society for Cell Biology under license from the author(s). Two months after publication it is available to the public under an Attribution–Noncommercial–Share Alike 3.0 Unported Creative Commons License (http://creativecommons.org/licenses/by-nc-sa/3.0).

"ASCB®," "The American Society for Cell Biology®," and "Molecular Biology of the Cell®" are registered trademarks of The American Society of Cell Biology.

much of its coiled-coil domain (Ciferri *et al.*, 2008), revealed that portions of the N termini of both Hec1 and Nuf2 fold into calponin homology (CH) domains, motifs well known for mediating binding to actin and, in fewer cases, to microtubules (Gimona *et al.*, 2002; Slep and Vale, 2007). The N terminus of Hec1 contains an additional motif that precedes the CH domain, referred to as the tail domain. This domain is highly basic and positively charged, and in humans is ~80 amino acids in length. Unfortunately, there are no structural data for this motif, which is predicted to be flexible and disordered (Wei *et al.*, 2007; Ciferri *et al.*, 2008; Guimaraes *et al.*, 2008). The Hec1 tail, however, is required for the efficient formation of stable kinetochore–microtubule attachments in cells (Guimaraes *et al.*, 2008; Miller *et al.*, 2008), and its removal results in a significant decrease in binding affinity of N-terminal Hec1 fragments or purified NDC80^{Bonsai} complexes for microtubules in vitro (Wei *et al.*, 2007; Ciferri *et al.*, 2008). The Hec1 tail is also likely involved in regulation of kinetochore–microtubule attachment stability, as multiple sites within this domain are phosphorylated in vitro by Aurora B kinase, which has been widely implicated in correcting kinetochore–microtubule attachment errors in mitosis by increasing kinetochore–microtubule turnover (Biggins and Murray, 2001; Tanaka *et al.*, 2002; Ditchfield *et al.*, 2003; Hauf *et al.*, 2003; Lampson and Kapoor, 2005; Cimini *et al.*, 2006; Pinsky *et al.*, 2006). This is supported by the finding that phosphorylation of the Hec1 tail domain by a purified Aurora kinase in vitro results in decreased binding affinity of the NDC80 complex for microtubules (Cheeseman *et al.*, 2006). Furthermore, in vivo studies have shown that the phosphorylation state of the Hec1 tail domain affects the stability of kinetochore–microtubule attachments. Specifically, expression of a nonphosphorylatable Hec1 tail domain mutant in cells results in hyperstable kinetochore–microtubule attachments (DeLuca *et al.*, 2006), whereas expression of phosphomimetic versions of Hec1 in cells results in unstable kinetochore–microtubule attachments (Guimaraes *et al.*, 2008; Welburn *et al.*, 2010).

Given the ability of CH domains to confer microtubule binding in known microtubule-associated proteins (Hayashi and Ikura, 2003; Dougherty *et al.*, 2005), it has been predicted that the ability of the NDC80 complex to mediate kinetochore–microtubule attachment in cells is largely facilitated by the Hec1 and Nuf2 CH domains. Structural data in combination with sequence analysis from various species reveal a conserved face of the Hec1-Nuf2 CH domain pair that is highly positively charged (Ciferri *et al.*, 2008). Charge reversal mutations (Lys to Glu) of even single amino acids within this conserved face in either Hec1 or Nuf2 resulted in a loss of high-affinity binding of NDC80 complexes to microtubules in vitro (Ciferri *et al.*, 2008). These findings have led to the prediction that both Hec1 and Nuf2 CH domains are essential for kinetochore–microtubule attachment in cells. Two recent cryo-electron microscopy studies, however, have suggested that, for microtubules decorated with recombinant NDC80 complexes in vitro, the CH domain of Hec1 directly interfaces the microtubule lattice, whereas the Nuf2 CH domain may not (Wilson-Kubalek *et al.*, 2008; Alushin *et al.*, 2010). Using a gene silence and rescue approach in HeLa cells, we investigated the respective contributions of the Hec1 and Nuf2 CH domains in the formation of kinetochore–microtubule attachments in vivo.

RESULTS

The Hec1 CH domain is required for chromosome alignment and stable kinetochore–microtubule attachment in cells

Endogenous Hec1 was depleted from HeLa cells using fluorescently labeled small interfering RNAs (siRNAs) directed to the 5′ untranslated region of human Hec1 (Supplemental Figure 1), and either wild-type (WT) Hec1 fused to green fluorescent protein (GFP) or mutant versions of Hec1-GFP were subsequently expressed. For all rescue experiments, kinetochore fluorescence intensities of the GFP fusion proteins were quantified, and only those cells whose average kinetochore fluorescence intensities fell into a defined experimental range were used (Supplemental Figure 2). Cells were fixed and assayed for their ability to align chromosomes at the spindle equator (Figure 1, A and B). Only cells that formed bipolar spindles were scored, and cells containing multipolar spindles were excluded. For each rescue experiment, the percentage of cells with multipolar spindles varied, but in all cases was under 25% (Supplemental Figure 3). Cells depleted of Hec1, as expected, failed to properly congress their chromosomes (Figure 1A), and 92% of transfected cells contained mostly unaligned chromosomes (defined as having no recognizable metaphase plate or a recognizable plate with >10 unaligned chromosomes). Cell populations rescued with WT Hec1-GFP, however, contained cells in all phases of mitosis, with 59% of cells exhibiting mostly aligned chromosomes (defined as having <5 chromosomes off a well-defined metaphase plate), 8% of cells exhibiting partially aligned chromosomes (defined as having 5–10 chromosomes off a metaphase plate), and 33% exhibiting mostly unaligned chromosomes (Figure 1B). To address the role of the Hec1 CH domain in kinetochore–microtubule attachment, we generated a charge reversal (positive to negative) point mutation within the conserved face of the CH domain at amino acid 166 from Lys to Asp (Hec1^{K166D}). This residue was chosen based on x-ray structures of the Hec1 CH domain (Wei *et al.*, 2007; Ciferri *et al.*, 2008) and the previous finding that a charge reversal mutation at this site decreased binding affinity of NDC80 complexes for microtubules by 54-fold in vitro (Ciferri *et al.*, 2008). Hec1^{K166D}-GFP failed to rescue the chromosome alignment defect in Hec1-depleted cells, and 89% of transfected cells exhibited mostly unaligned chromosomes (Figure 1, A and B). To determine whether stable kinetochore–microtubule attachments were able to form, cells were subjected to a cold-induced microtubule depolymerization assay. In this assay, most nonkinetochore microtubules are depolymerized, and microtubules embedded by their plus ends into kinetochores are selectively stabilized. Cells rescued with WT Hec1-GFP retained abundant kinetochore fibers, whereas those rescued with Hec1^{K166D}-GFP did not (Figure 1C). Quantification revealed a 68% decrease in cold-stable microtubule polymer in cells rescued with Hec1^{K166D}-GFP when compared with cells rescued with WT Hec1-GFP, which was similar to the decrease measured in cells depleted of Hec1 (Figure 1D). These results indicate that the conserved, charged surface of the Hec1 CH domain is required for the formation of stable kinetochore–microtubule attachments in HeLa cells.

It has been previously reported that the N-terminal tail domain of Hec1 is required for the generation of stable kinetochore–microtubule attachments in cells (Guimaraes *et al.*, 2008; Miller *et al.*, 2008). Furthermore, cultured cells expressing Hec1 mutants in which multiple amino acids within the tail were mutated to mimic phosphorylation (Ser or Thr to Asp) failed to form stable kinetochore–microtubule attachments (Guimaraes *et al.*, 2008; Welburn *et al.*, 2010). To compare the phenotypes of HeLa cells rescued with a Hec1 CH domain mutant versus a tail domain mutant, we rescued Hec1-depleted HeLa cells with 9D Hec1-GFP, a mutant in which nine amino acids (Ser or Thr) within the tail were mutated to Asp to mimic phosphorylation. As expected, cells expressing 9D Hec1-GFP exhibited defects in aligning their chromosomes (Figure 1A); 66% of cells exhibited mostly unaligned chromosomes, 14% of cells exhibited partially aligned chromosomes, and 20% exhibited mostly aligned chromosomes (Figure 1B). Although these cells

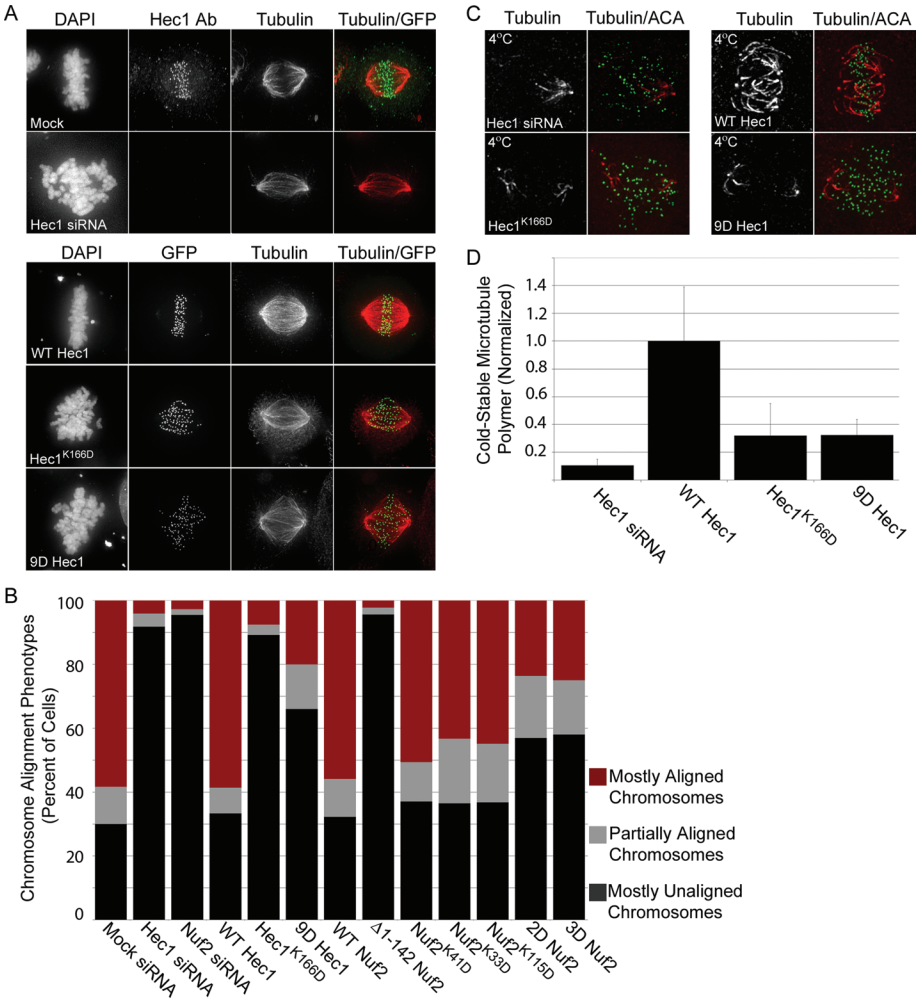

FIGURE 1: Stable kinetochore–microtubule attachment depends on the charged face of the Hec1 CH domain. (A) Immunofluorescence images showing HeLa cells depleted of Hec1 and rescued with mutant versions. The upper panels show a control cell and a cell depleted of endogenous Hec1. The lower panels show cells depleted of endogenous Hec1 and rescued with either WT Hec1 or a Hec1 mutant fused to GFP. (B) Quantification of chromosome alignment phenotypes in cells depleted of Hec1 or Nuf2 and cells rescued with Hec1 or Nuf2 GFP fusions. Cells with mostly aligned chromosomes (red) exhibited <5 chromosomes off of a well-formed metaphase plate, cells with partially aligned chromosomes (gray) exhibited 5–10 chromosomes off of a metaphase plate, and cells with mostly unaligned chromosomes (black) exhibited either no chromosome alignment or >10 chromosomes off of a metaphase plate. For each condition, at least 90 cells were scored. (C) Images of cells subjected to a cold-induced microtubule-depolymerization assay and immunostained with tubulin and ACA antibodies (recognizing CENP-A, -B, and -C). Cells depleted of Hec1 and cells depleted of Hec1 and rescued with either WT or mutant GFP fusions are shown. (D) Quantification of microtubule fluorescence intensity after cold-induced microtubule depolymerization. For each condition, spindles from at least 10 cells were measured.

exhibited a clear defect in chromosome alignment, we noted that a small population could align chromosomes at the spindle equator. To determine whether stable kinetochore–microtubules were able to form in cells rescued with 9D Hec1-GFP, we carried out a cold-induced microtubule depolymerization assay. Cells rescued with 9D Hec1-GFP did not retain high levels of microtubule polymer after incubation in ice-cold media (Figure 1, C and D), suggesting that kinetochore–microtubule attachment was indeed impaired. These results demonstrate that both the tail and the CH domains of Hec1 are important for the formation of stable kinetochore–microtubule attachments in HeLa cells, but disruption of the CH domain results in a somewhat more severe defect in chromosome alignment.

To determine the fate of cells rescued with Hec1 mutants, we performed live-cell imaging of HeLa cells transiently transfected with mCherry-histone H2B to visualize chromosomes. Each cell included in the analysis was confirmed to be transfected with Hec1 siRNA (detected by Cy5 fluorescence). For all live-cell time-lapse imaging experiments, the GFP fluorescence intensity at kinetochores was quantified, and only those cells whose average kinetochore fluorescence intensities fell into a defined experimental range were used (Supplemental Figure 4). The majority of cells depleted of endogenous Hec1 and rescued with WT Hec1-GFP formed metaphase plates and entered anaphase with aligned chromosomes (Figure 2; Supplemental Movie 1). The average time from nuclear envelope breakdown to anaphase onset was 31 ± 5 min. By contrast, 17 of 18 cells rescued with Hec1^{K166D}-GFP failed to align their chromosomes and arrested in a prometaphase-like state for >5 h (Figure 2; Supplemental Movie 2). Cells rescued with the phosphomimetic tail domain mutant 9D Hec1-GFP also experienced severe defects in chromosome segregation (Figure 2). Specifically, of 16 cells filmed, 13 failed to align chromosomes and remained arrested in a prometaphase-like state for >5 h (Figure 2; Supplemental Movie 3). Results from these experiments demonstrate that both the tail and CH domains of Hec1 are required for correct chromosome alignment and timely progression through mitosis.

The Nuf2 CH domain is required for timely progression through mitosis

We next investigated the role of the Nuf2 CH domain in chromosome alignment and kinetochore–microtubule attachment using the silence and rescue system described above for Hec1. As expected, HeLa cells depleted of Nuf2, which results in a concomitant depletion of Hec1 (DeLuca *et al.*, 2003; Hori *et al.*, 2003), failed to align their chromosomes, and 95% of transfected cells exhibited mostly unaligned chromosomes (Figures 1B and 3A). Expression of WT Nuf2-GFP in Nuf2-depleted cells rescued the chromosome alignment defect; 56% of cells exhibited mostly aligned chromosomes, 12% of cells exhibited partially aligned chromosomes, and 32% exhibited mostly unaligned chromosomes. By contrast, cells rescued with a Nuf2 mutant deleted of its entire CH domain (Δ1–142 Nuf2) fused to GFP, failed to restore normal chromosome alignment, and 96% of cells expressing Δ1–142 Nuf2-GFP exhibited mostly unaligned chromosomes (Figures 1B and 3A). We reasoned that this may not be an appropriate approach to specifically test the role of the Nuf2 CH domain in mitotic functions, as removal of the entire domain likely affects the structure or positioning of the remaining Hec1 N terminus. To more precisely address the role of the Nuf2 CH domain in kinetochore–microtubule

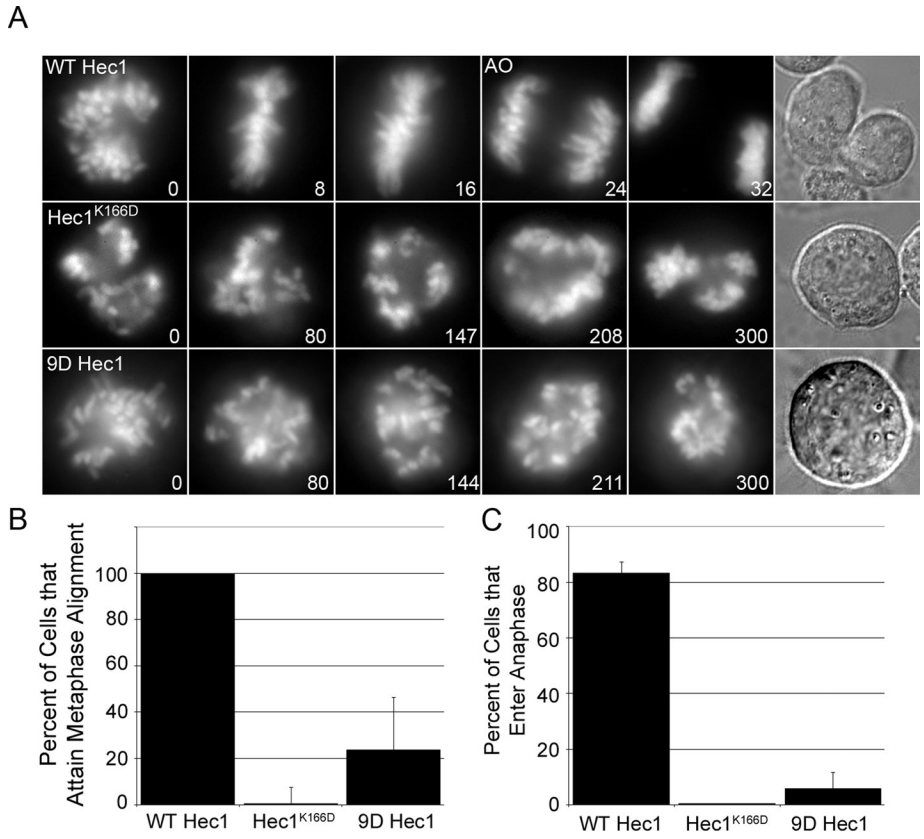

FIGURE 2: Cells rescued with a Hec1 CH domain charge reversal mutant arrest in mitosis with unaligned chromosomes. (A) Still images from time-lapse acquisitions of HeLa cells depleted of endogenous Hec1 and rescued with either WT Hec1-GFP or Hec1 mutants fused to GFP. Time is shown in minutes, and anaphase onset (AO) is indicated for the WT Hec1-GFP-rescued cell that entered anaphase. The DIC image shows the time point corresponding to the final mCherry image. (B) Quantification of metaphase plate formation during live cell imaging. Bar graph represents the percent of cells that attained metaphase alignment at some point during time-lapse imaging. (C) Quantification of anaphase entry during live cell imaging. Bar graph represents the percent of cells that entered anaphase during time-lapse imaging. All cells were filmed for 5 h except those rescued with WT Hec1, which were filmed for 2 h. Error bars in (B) and (C) represent SD across at least 2 independent experiments. The n values for each experiment are as follows: WT Hec1, 12 cells; Hec1^{K166D}, 18 cells; 9D Hec1, 17 cells.

attachment, we generated a single charge reversal mutation in the conserved, positively charged face of the CH domain (Ciferri *et al.*, 2008), similar to the strategy used for Hec1. We mutated Lys115 to Asp (Nuf2^{K115D}), due to the previous finding that a charge reversal mutation at this site reduced the affinity of NDC80 complexes for microtubules in vitro by 46-fold (Ciferri *et al.*, 2008). Surprisingly, cells rescued with Nuf2^{K115D}-GFP were able to align their chromosomes nearly as well as those cells rescued with WT Nuf2-GFP (Figures 1B and 3A). We next generated single charge reversal mutations at Lys33 and at Lys41, which also reside within the conserved face of the Nuf2 CH domain. Cells depleted of endogenous Nuf2 and rescued with either Nuf2^{K33D} or Nuf2^{K41D} were also able to align their chromosomes nearly as well as cells rescued with WT Nuf2-GFP, indicating that single amino acid charge reversal mutations within the Nuf2 CH domain are not sufficient to disrupt chromosome alignment.

To more severely disrupt the charged face of the Nuf2 CH domain, we generated mutants in which two or three of the Lys residues were mutated to Asp, termed 2D Nuf2-GFP (Lys33 and Lys41 mutated to Asp) and 3D Nuf2-GFP (Lys33, Lys41, and Lys115 mutated to Asp), respectively. In each case, the ability of cells to align chromosomes was impaired when compared with cells rescued with mutants containing a single amino acid change. Specifically, in cells rescued with 2D Nuf2-GFP or 3D Nuf2-GFP, only ~25% of the fixed cells scored were able to align their chromosomes, compared with ~40% for any of the single charge reversal mutants (Figures 1B and 3A). Of note, the chromosome alignment phenotypes for cells expressing the 2D or 3D Nuf2 CH domain mutants were significantly less severe than those phenotypes in cells expressing a Hec1 CH domain mutant with a single amino acid change. Due to this, we tested whether the kinetochore–microtubule attachments in cells rescued with Nuf2 CH domain mutants with partially aligned or mostly aligned chromosomes were stable. We first quantified the level of cold-stable microtubule polymer in these cells and found that those rescued with a mutant containing a single amino acid change (Nuf2^{K115D}-GFP) or with three amino acid changes (3D Nuf2-GFP) retained near-WT levels of cold-stable microtubule polymer (Figure 3, B and C). To further assess kinetochore–microtubule attachment stability, we measured the distances between sister kinetochores on bioriented chromosomes. The average interkinetochore distance for sister kinetochores on bioriented chromosomes in cells rescued with WT Nuf2-GFP was 1.34 ± 0.24 μm (compared with 0.63 ± 0.15 μm in prophase, at "rest length"). By contrast, the average interkinetochore distance of sister pairs on bioriented chromosomes in cells rescued with Nuf2^{K115D}-GFP was 1.15 ± 0.19 μm, and 0.97 ± 0.14 μm in cells rescued with 3D Nuf2-GFP (Figure 3D). Although modest, these decreases in average interkinetochore distance (14% and 28%, respectively, from WT) are statistically significant ($p < 0.0001$), indicating that mutation of the conserved face of the Nuf2 CH domain results in a defect in generating WT kinetochore tension on bioriented chromosomes.

To determine the fate of cells rescued with Nuf2-GFP fusion proteins, we followed Nuf2-depleted cells rescued with WT Nuf2-GFP or mutant versions of Nuf2-GFP via time-lapse microscopy. Cells depleted of endogenous Nuf2 and rescued with WT Nuf2-GFP properly aligned chromosomes at the spindle equator and entered anaphase in an average of 40 ± 8 min (Figure 4; Supplemental Movie 4). As predicted from our fixed cell analysis, cells rescued with Δ1–142 Nuf2-GFP failed to align chromosomes at the spindle equator, and all cells imaged arrested for >5 h in a prometaphase-like state (Figure 4; Supplemental Movie 5). By contrast, most cells rescued with the single Lys-to-Asp mutants (Nuf2^{K115D}-GFP, Nuf2^{K33D}-GFP, and Nuf2^{K41D}-GFP) were able to align their chromosomes and generate metaphase plates (Figure 4; Supplemental Movies 6–8, respectively). In many cases, alignment was transient, with individual chromosomes leaving and returning to the spindle equator, or in some cases, the entire plate would disassemble and eventually reassemble. As observed in the fixed cell analysis, chromosome

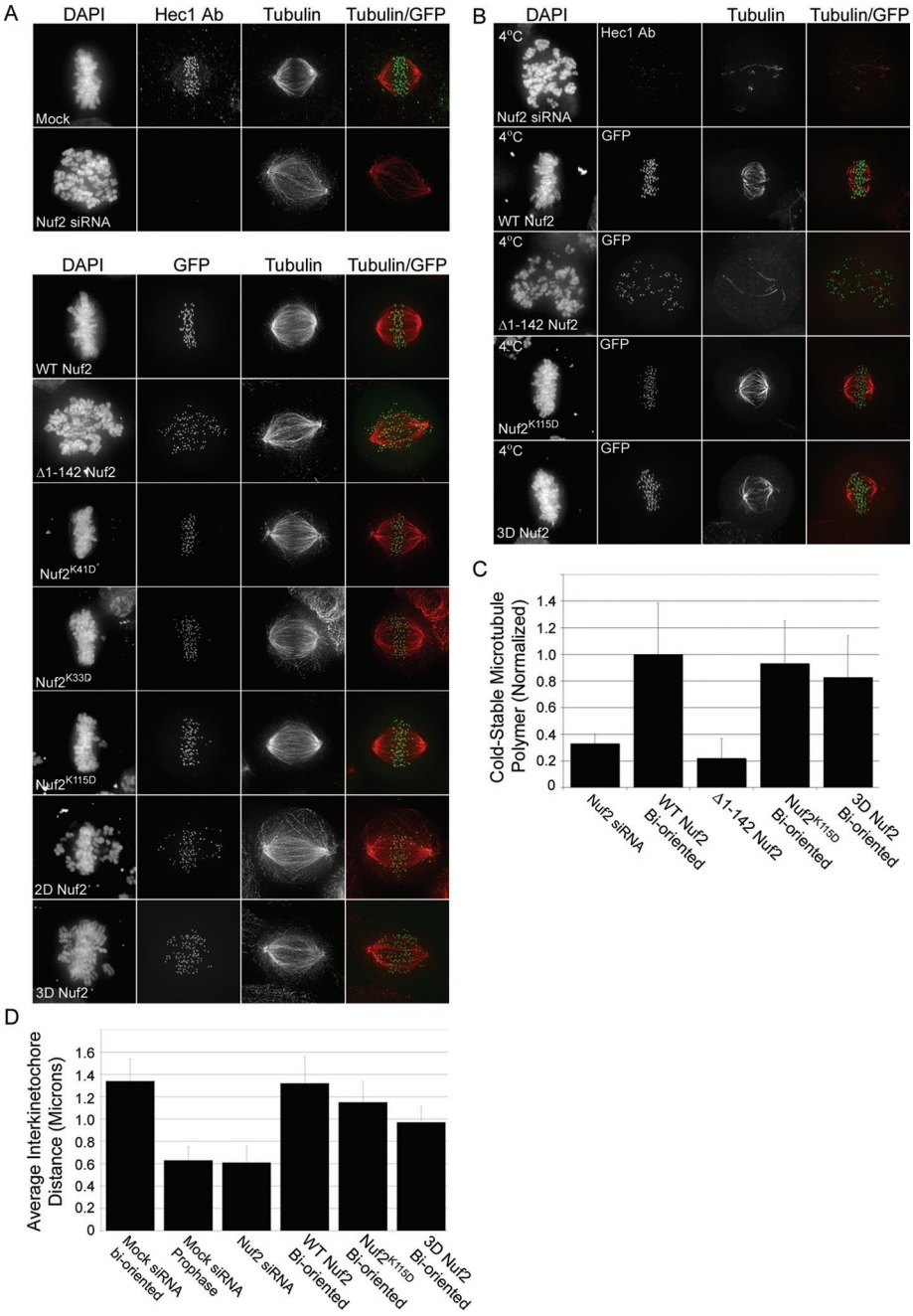

FIGURE 3: The charged face of the Nuf2 CH domain is not required for the formation of stable kinetochore–microtubule attachments. (A) Immunofluorescence images showing HeLa cells depleted of Nuf2 and rescued with various mutant versions. The upper panels show a control cell and a cell depleted of endogenous Nuf2 stained with Hec1 and tubulin antibodies. The lower panels show cells depleted of endogenous Nuf2 and rescued with either WT Nuf2 or a Nuf2 mutant fused to GFP. For the 2D Nuf2 mutant, two Lys-to-Asp substitutions were made at amino acid positions 33 and 41; the 3D Nuf2 mutant contains three Lys-to-Asp substitutions at amino acid positions 33, 41, and 115. (B) Images of cells subjected to a cold-induced microtubule-depolymerization assay and immunostained with tubulin antibodies, DAPI, and, in Nuf2-depleted cells, Hec1 antibodies. Cells depleted of Nuf2 alone and cells depleted of Nuf2 and rescued with either WT or mutant GFP fusions are shown. (C) Quantification of microtubule fluorescence intensity after cold-induced microtubule depolymerization. For each condition, spindles from at least 10 cells were measured. (D) Quantification of interkinetochore distances, which were measured from GFP-centroid to GFP-centroid in cells rescued with Nuf2-GFP fusion proteins. In cells depleted of Nuf2, interkinetochore distances were measured from ACA-centroid to ACA-centroid. For cells depleted of endogenous Nuf2 and rescued with GFP-fusions, kinetochores from bioriented chromosomes were measured.

alignment defects were more severe in cells expressing 2D Nuf2-GFP and 3D Nuf2-GFP, but a significant population of these cells (60% and 32%, respectively) were able to align chromosomes at the spindle equator at some point during filming (Figure 4; Supplemental Movies 9 and 10). This is in contrast to cells depleted of Hec1 and rescued with the single charge reversal mutant, Hec1^{K166D}-GFP, in which no chromosome alignment was observed (Figure 2).

Although cells rescued with the Nuf2 CH domain mutants were able to align their chromosomes (to varying degrees), they failed to enter anaphase in a timely manner. Specifically, only 42%, 47%, and 21% of cells rescued with the single charge reversal mutants Nuf2^{K115D}-GFP, Nuf2^{K33D}-GFP, or Nuf2^{K41D}-GFP, respectively, entered anaphase during the 5 h of imaging. In addition, the cells that did enter anaphase did so with an average delay of ~40 min when compared with cells rescued with WT Nuf2-GFP (data not shown). Similarly, only 16% and 26% of cells rescued with 2D Nuf2-GFP or 3D Nuf2-GFP, respectively, entered anaphase during the 5-h time lapse, and these cells did so with an average delay of ~90 min when compared with cells rescued with WT Nuf2-GFP (data not shown). Together, these results suggest that the conserved, charged face of the Nuf2 CH domain is not absolutely required for formation of stable kinetochore–microtubule attachments but is needed to generate WT tension across sister kinetochore pairs and for timely entry into anaphase.

Nuf2 CH domain mutants do not affect recruitment of kinetochore outer domain proteins

Due to the distinct phenotypes observed in cells rescued with Nuf2 CH domain mutants compared with those rescued with Hec1 mutants, we tested whether cells expressing Nuf2 CH domain mutants were defective in recruiting kinetochore outer domain proteins. As expected, Hec1 was absent from kinetochores in Nuf2-depleted cells (Figure 5) but present on kinetochores in cells rescued with either WT Nuf2-GFP or 3D Nuf2-GFP. We next tested for the presence of Ska complex proteins, because cells depleted of these proteins have been shown to exhibit defects similar to those we observed in cells rescued with Nuf2^{K115D}-GFP or 3D Nuf2-GFP (Hanisch *et al.*, 2006; Daum *et al.*, 2009; Gaitanos *et al.*, 2009; Raaijmakers *et al.*, 2009; Theis *et al.*, 2009; Welburn *et al.*, 2009). As previously demonstrated, Ska1 and Rama1/Ska3 were absent from kinetochores in cells depleted of Nuf2

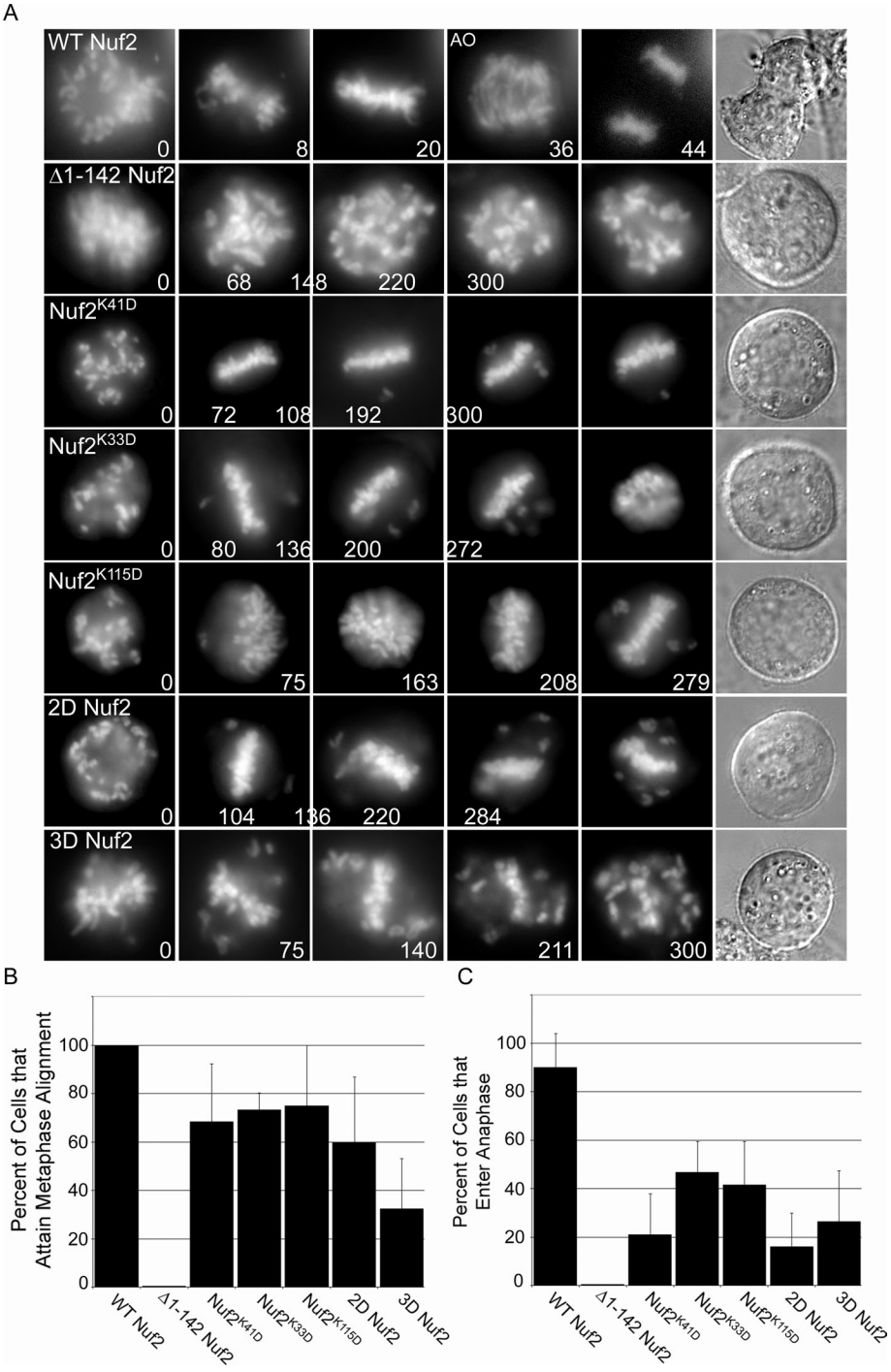

FIGURE 4: Cells rescued with Nuf2 CH domain charge reversal mutants arrest in mitosis with at least partially aligned chromosomes. (A) Still images from time-lapse acquisitions of HeLa cells depleted of endogenous Nuf2 and rescued with either WT Nuf2-GFP or Nuf2 mutants fused to GFP. Time is shown in minutes, and anaphase onset (AO) is indicated for the cell expressing WT Nuf2-GFP that entered anaphase. The DIC image shows the time-point corresponding to the final mCherry image. (B) Quantification of metaphase plate formation during live cell imaging. Bar graph represents the percent of cells that attained metaphase alignment at some point during time-lapse imaging. (C) Quantification of anaphase entry during live cell imaging. Bar graph represents the percent of cells that entered anaphase during time-lapse imaging. All cells were filmed for 5 h, except those rescued with WT Nuf2, which were filmed for 2 h. Error bars in (B) and (C) represent SD across at least 2 independent experiments. The n values for each experiment are as follows: WT Nuf2, 10 cells; Δ1–142 Nuf2, 8 cells; $Nuf2^{K41D}$, 19 cells; $Nuf2^{K33D}$, 15 cells; $Nuf2^{K115D}$, 12 cells; 2D Nuf2, 25 cells; 3D Nuf2, 34 cells.

(Hanisch *et al.*, 2006; Raaijmakers *et al.*, 2009; Welburn *et al.*, 2009). However, both Ska1 and Rama1/Ska3 were present at kinetochores in cells rescued with WT Nuf2-GFP or 3D Nuf2-GFP (Figure 5). The outer domain protein CLASP1, which was also absent from kinetochores in cells depleted of Nuf2, was present at kinetochores in cells rescued with WT Nuf2-GFP or 3D Nuf2-GFP (Figure 5). Similar results were found for ZW10, which was absent from kinetochores in cells depleted of Nuf2, but present at kinetochores in cells rescued with WT Nuf2-GFP or 3D Nuf2-GFP (Figure 5). Finally, CENP-E and KNL1 were present at kinetochores in Nuf2-depleted cells and in cells rescued with WT Nuf2-GFP and 3D Nuf2-GFP (Figure 5). These results suggest that the defects observed in cells rescued with the Nuf2 CH domain mutants are not due to impaired recruitment of kinetochore outer domain proteins.

Distinct roles for Nuf2 and Hec1 CH domains in kinetochore function

Phosphorylation of the Hec1 tail domain has been suggested to play an important role in the regulation of kinetochore–microtubule attachment (Cheeseman *et al.*, 2006; DeLuca *et al.*, 2006). Cells expressing nonphosphorylatable tail domain mutants of Hec1 form stable kinetochore–microtubule attachments but exhibit an increased rate of attachment errors (DeLuca *et al.*, 2006), suggesting that prevention of phosphorylation of the Hec1 tail results in the generation of hyperstable kinetochore–microtubule attachments. We wanted to test whether a nonphosphorylatable tail domain mutant of Hec1 could rescue the attachment defects observed in cells rescued with the Hec1 and Nuf2 CH domain mutants. We first time-lapse imaged HeLa cells depleted of endogenous Hec1 and rescued with 9A Hec1-GFP, a mutant version of Hec1 in which all 9 putative Aurora B kinase phosphorylation sites (Ser or Thr) in the tail domain were mutated to Ala to prevent phosphorylation. The majority of cells rescued with 9A Hec1-GFP were unable to completely align their chromosomes, but 19 of 20 cells filmed entered anaphase in an average of 75 ± 30 min after nuclear envelope breakdown with multiple lagging chromosomes (Figure 6; Supplemental Movie 11). Fixed-cell analysis of cells rescued with 9A Hec1-GFP demonstrated that stable kinetochore–microtubule attachments were able to form, and interkinetochore distances of sister kinetochore pairs on bioriented chromosomes were increased

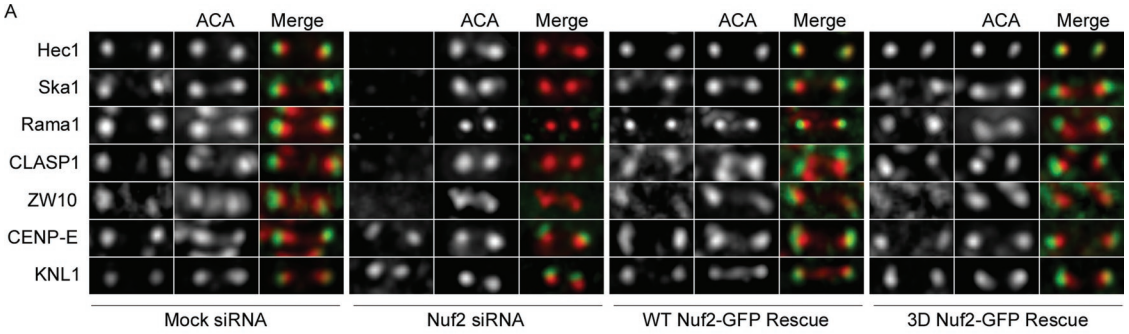

B

	Mock siRNA	Nuf2 siRNA	WT Nuf2 Rescue	3D Nuf2 Rescue
Hec1	+	-	+	+
Ska1	+	-	+	+
Rama1	+	-	+	+
CLASP1	+	-	+	+
ZW10	+	-	+	+
CENP-E	+	+	+	+
KNL1	+	+	+	+

FIGURE 5: Charge reversal mutations within the Nuf2 CH domain do not affect recruitment of outer kinetochore proteins. (A) Images showing single kinetochore pairs from control cells, Nuf2-depleted cells, cells rescued with WT Nuf2-GFP, and cells rescued with 3D Nuf2-GFP. For each series, the first panel shows immunostaining for the antibody listed on the far left. ACA staining is shown as well a merge of ACA staining with each test antibody. (B) Chart summarizing immunofluorescence data shown in (A).

from those measured in metaphase cells expressing WT Hec1-GFP (data not shown).

We next designed a 9A Hec1^{K166D}-GFP mutant and used this to rescue cells depleted of endogenous Hec1. The nonphosphorylatable Hec1 tail failed to rescue the attachment defect resulting from the K166D mutation, and cells remained arrested in mitosis rather than entering anaphase as did the cells rescued with 9A Hec1-GFP (Figure 6; Supplemental Movie 12). To determine whether the nonphosphorylatable Hec1 tail could compensate for the defects observed in cells rescued with the Nuf2 CH domain mutants, we carried out double silence and rescue experiments, in which siRNAs directed to the sequences of both Nuf2 and Hec1 were transfected into HeLa cells, and cells were subsequently rescued with Nuf2^{K115D}-GFP and either WT Hec1 or 9A Hec1. As shown in Figure 6, time-lapse imaging reveals that cells rescued with Nuf2^{K115D}-GFP and WT Hec1 exhibited a phenotype similar to that of cells rescued with Nuf2^{K115D}-GFP alone, and the majority of cells arrested in mitosis for >5 h (Figure 6; Supplemental Movie 14). We did note that when compared to the Nuf2-alone silence and rescue experiments (Figure 4C), there was a modest decrease in the average number of cells that entered anaphase in the double silence and rescue experiments. By contrast, most cells rescued with Nuf2^{K115D}-GFP and 9A Hec1 did not arrest (16 of 19 cells), but instead initiated anaphase in an average of 55 ± 34 min (Figure 6; Supplemental Movie 15). Not unexpectedly, many cells exhibited one or multiple lagging chromosomes in anaphase (data not shown). Similar results were observed in cells depleted of Nuf2 and Hec1 and rescued with 3D Nuf2-GFP and 9A Hec1. Here, an increased number of cells (44%) entered anaphase when compared with cells depleted of Nuf2 and Hec1 and rescued with 3D Nuf2-GFP and WT Hec1 (14%) (Figure 6; Supplemental Movies 16 and 17). Similar to cells rescued with Nuf2^{K115D}-GFP and 9A Hec1, we often observed lagging chromosomes in cells rescued with 3D Nuf2-GFP and 9A Hec1 that entered anaphase. These results suggest that the Nuf2 CH domain is not absolutely required for the formation of tension-generating, end-on kinetochore–microtubule attachments. The Hec1 CH domain, together with the Hec1 tail domain, can generate sufficiently stable kinetochore–microtubule attachments to silence the spindle assembly checkpoint.

DISCUSSION

We find that mutating a single Lys residue within the CH domain of Hec1 (Lys166 to Asp) severely perturbs kinetochore–microtubule attachment stability in vivo. This is not surprising, since recombinantly expressed, purified NDC80^{Bonsai} complexes containing a charge reversal mutation at this residue have been shown to bind microtubules in vitro with 54-fold less affinity than WT NDC80^{Bonsai} complexes (Ciferri *et al.*, 2008). We also demonstrated that a nonphosphorylatable Hec1 tail-domain mutant, which has been previously shown to induce hyperstable kinetochore–microtubule attachments (DeLuca *et al.*, 2006), was not able to rescue the Hec1^{K166D} phenotype, further suggesting that the CH domain of Hec1 is absolutely essential for high-affinity kinetochore–microtubule binding. In contrast, we found that mutating single Lys residues in the CH domain of Nuf2 had a significantly less severe effect on the formation of stable kinetochore–microtubule attachments. The same mutations, however, resulted in a decrease in binding affinity of purified NDC80^{Bonsai} complexes in vitro. Specifically, a charge reversal mutation at Lys115 decreased the microtubule binding affinity 46-fold, whereas mutations at Lys33 and Lys41 resulted in a 9-fold and 6-fold decrease in affinity, respectively (Ciferri *et al.*, 2008). In our study, cells expressing Nuf2 CH domain charge reversal mutants were able to generate stable kinetochore–microtubule attachments and exhibited only a partial loss of interkinetochore tension and cold-stable microtubule polymer. Furthermore, the partial loss of kinetochore–microtubule attachment stability could be compensated for by coexpression of a nonphosphorylatable Hec1 tail domain mutant. Our results support a model in which the Hec1 protein interfaces the microtubule lattice to generate high-affinity kinetochore–microtubule attachments, whereas the Nuf2 protein does not.

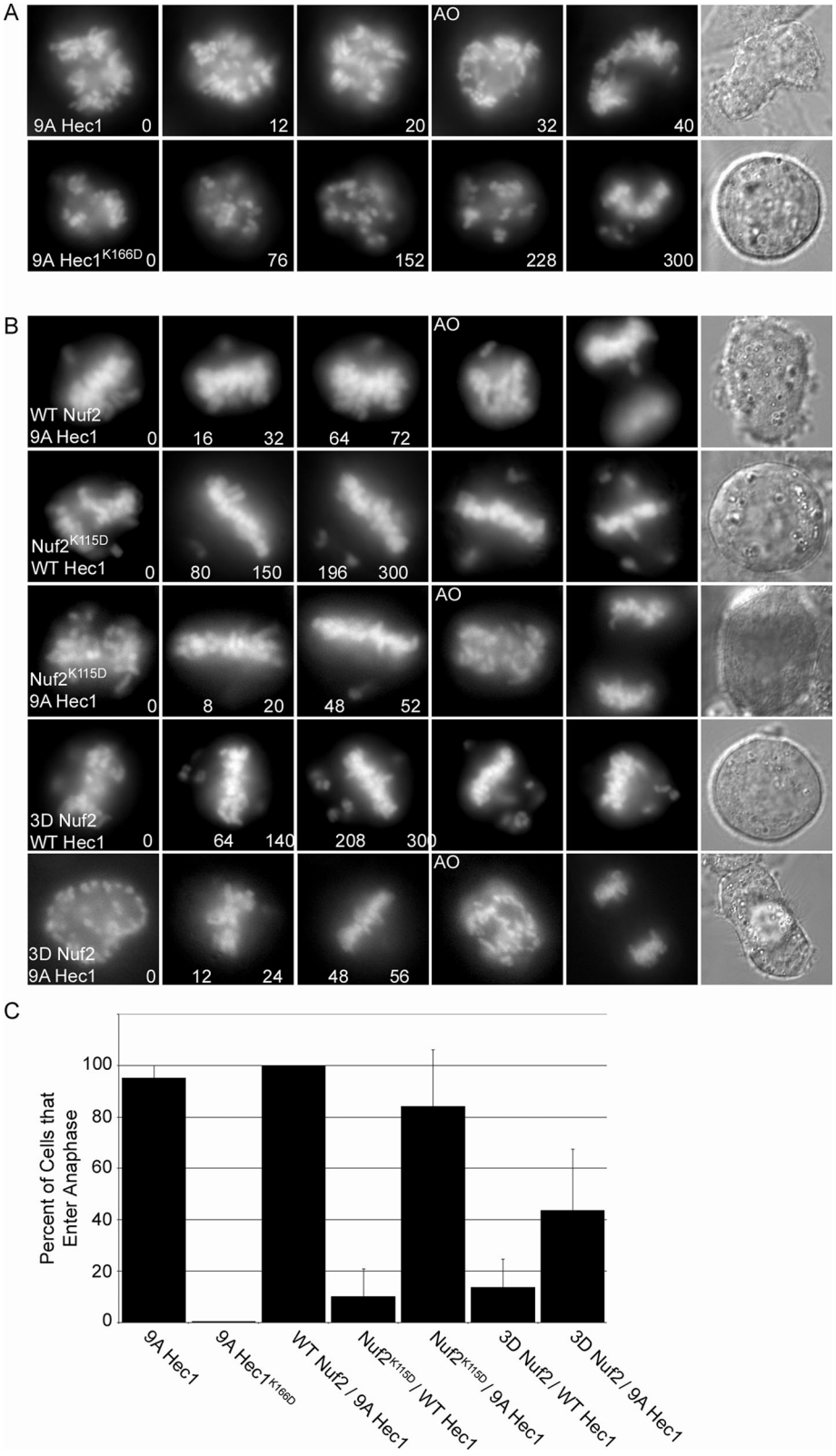

FIGURE 6: Expression of a nonphosphorylatable Hec1 tail domain overcomes the mitotic arrest observed in cells rescued with a Nuf2 CH domain charge reversal mutant, but not a Hec1 CH domain charge reversal mutant. (A) Still images from time-lapse acquisitions of HeLa cells depleted of endogenous Hec1 and rescued with either 9A Hec1-GFP or 9A Hec1^{K166D}-GFP. The DIC image shows the time point corresponding to the final mCherry image. (B) Still images from time-lapse acquisitions of HeLa cells depleted of endogenous Nuf2 and Hec1 using siRNAs targeted to both Nuf2 and Hec1 genes, and rescued with either WT Nuf2-GFP or a mutant Nuf2-GFP containing Lys-to-Asp mutations in the CH domain, and either WT Hec1- or 9A Hec1-GFP. Time is shown in minutes, and anaphase onset (AO) is indicated for cells that enter anaphase in (A) and (B). (C) Quantification of anaphase entry during live cell imaging. Bar graph represents the percent of cells that entered anaphase during time-lapse imaging. All cells were filmed for 5 h. Error bars represent SD across at least 2 independent experiments. The n values for each experiment are as follows: 9A Hec1, 20 cells; 9A Hec1^{K166D}, 18 cells; WT Nuf2/9A Hec1, 28 cells; Nuf2^{K115D}/ WT Hec1, 20 cells; Nuf2^{K115D}/9A Hec1, 19 cells; 3D Nuf2/WT Hec1, 29 cells; 3D Nuf2/9A Hec1, 39 cells.

Our results are consistent with two recently published studies that generated models of the NDC80 complex–microtubule interface based on cryo-electron microscopy data fitted to the crystal structures of tubulin and the CH domains of Hec1 and Nuf2 (Wilson-Kubalek *et al.*, 2008; Alushin *et al.*, 2010). These models suggest that the interface between the microtubule lattice and the NDC80 complex is made up of only a small region within the Hec1 CH domain, and this region includes Lys at position 166. In both reconstructed models, the Nuf2 CH domain does not interface the microtubule, but faces away from the lattice (Wilson-Kubalek *et al.*, 2008; Alushin *et al.*, 2010). The Nuf2 Lys residues that were mutated in our study (Lys33, Lys41, and Lys115) lie within the region of the Nuf2 CH domain that faces away from the microtubule lattice according to both of these studies, which may explain the difference in severity of phenotypes exhibited by cells expressing Hec1 and Nuf2 CH domain mutants.

Although the Nuf2 CH domain is not likely required for direct microtubule binding, cells expressing Nuf2 CH domain mutants do experience mitotic defects. Specifically, sister kinetochores fail to generate WT interkinetochore tension, and cells arrest in mitosis with aligned or partially aligned chromosomes. One possibility is that the Nuf2 CH domain serves to recruit other outer kinetochore proteins. To address this, we tested the localization of outer kinetochore proteins known to be important at the microtubule interface. Of the proteins investigated, which included Ska1, Rama1, CLASP1, ZW10, CENP-E, and KNL1, all localized to kinetochores in cells expressing the 3D Nuf2 CH domain mutant. This suggests that lack of protein recruitment is not likely responsible for the observed phenotypes; however, it is possible that the Nuf2 CH domain recruits an outer kinetochore protein required for

the generation of WT interkinetochore tension that was not tested.

A second possibility is that the Nuf2 CH domain plays a role in properly oligomerizing NDC80 complexes at the kinetochore or tethering NDC80 complexes to one another so that optimal tension-generating kinetochore–microtubule associations can be formed. It has been demonstrated in vitro that NDC80 complex binding to microtubules is cooperative, and oligomerization of complexes is required for high-affinity binding (Cheeseman *et al.*, 2006; Ciferri *et al.*, 2008; Powers *et al.*, 2009; Alushin *et al.*, 2010). If the Nuf2 CH domain is required for such oligomerization, it could provide an explanation for the phenotype severity differences observed between in vitro and in vivo experiments with Nuf2 CH domain charge reversal mutants. The defects in cells may be less severe because the kinetochore serves to position NDC80 complexes into a specific geometry in relation to the microtubule lattice, reducing the need for explicit oligomerization of NDC80 complexes to facilitate kinetochore–microtubule binding. As kinetochore–microtubule attachments become stabilized during metaphase, however, oligomerization of adjacent NDC80 complexes may be critical for the generation of WT levels of interkinetochore tension. For NDC80 complex–microtubule binding studies carried out in vitro, the complexes are not specifically arranged and concentrated by a structure such as the kinetochore; therefore, the requirement for domains that facilitate oligomerization may be more stringent. Because of this, mutation of such domains would likely result in a significant loss in high-affinity microtubule binding in vitro.

MATERIALS AND METHODS

Cell culture

HeLa cells were cultured in DMEM (Invitrogen, Carlsbad, CA) supplemented with 10% fetal bovine serum (FBS) (Atlanta Biologicals, Norcross, GA) and 1% antibiotic/antimycotic solution at 37°C in 5% CO_2. Cells were plated at 50% confluency 24 h prior to transfection on acid-washed glass coverslips for immunofluorescence or on glass-bottomed dishes for live cell imaging (MatTek, Ashland, MA). For cold-induced depolymerization assays, cells on coverslips were incubated in ice-cold DMEM for 15 min on ice, then prepared for immunofluorescence as described below.

Transfection

siRNAs against Nuf2 (DeLuca *et al.*, 2002) and Hec1 (5′-AACCCTGGGTCGTGTCAGGAA-3′) were purchased from QIAGEN (Valencia, CA). Both siRNAs were tagged with a 3′ Cy5 label. For siRNA transfection, 6 µl Oligofectamine (Invitrogen) was added to 48 µl OptiMem (Invitrogen), and the tube was flicked intermittently for 5 min. To this, 8 µl of 20 µM siRNA and 200 µl of OptiMem were added and incubated for 30 min with periodic flicking of the tube. After incubation, the siRNA solution was added to 1 ml OptiMem + 10% FBS and added to cells on coverslips in six-well dishes or in glass-bottom dishes. Twenty-four hours posttransfection, 1 ml OptiMem (supplemented with 10% FBS) was added to the cells; cells were assayed at 48 h posttransfection. For silence and rescue experiments, cells were transfected with plasmid DNA using FuGene6 (Roche Diagnostics, Indianapolis, IN) 24 h after transfection using siRNA. For these experiments, 4 µl FuGene6 and 96 µl OptiMem were incubated for 5 min with regular flicking of the tube, and 1 µg plasmid DNA was added and incubated for 30 min with periodic flicking of the tube. The DNA solution was added to 1 ml OptiMem + 10% FBS and added to cells that had been previously transfected with siRNA. Cells were assayed 24 h following DNA transfection.

Electroporation

For live cell imaging experiments, a combination of lipid-based transfection and electroporation using a Nucleofector apparatus (Lonza, Cologne, Germany) was used. Cells were seeded in T25 flasks and grown to 50% confluency. Cells were transfected with Nuf2 or Hec1 siRNA using Oligofectamine (as described above). Eight hours posttransfection, cells were trypsinized and counted to ensure that 10^6 cells were used for each reaction. Cells were harvested and pelleted by centrifugation. The cell pellet was resuspended in 100 µl of Solution L (Lonza) per 10^6 cells. DNA constructs to be transfected were aliquoted at appropriate volumes to yield 4–8 µg per transfection into Eppendorf tubes. To each tube, 100 µl of cell suspension was added; the mixture was then added to an electroporation cuvette (Lonza). Cells were electroporated using program number V-001 and plated onto acid-washed coverslips or into glass-bottomed dishes in OptiMem + 10% FBS. Cells were analyzed 24 h postelectroporation.

Immunofluorescence and image acquisition

HeLa cells were initially fixed for 10 s in 4% paraformaldehyde (preheated to 37°C) followed by a 5-min permeabilization in fresh PHEM buffer (60 mM PIPES, 25 mM HEPES, 10 mM EGTA, 2 mM MgCl2, pH 7.0) + 0.5% Triton-X 100 at 37°C. Cells were then fixed for 20 min at room temperature in 4% paraformaldehyde (solution preheated to 37°C) in PHEM buffer and rinsed in PHEM + 0.1% Triton-X 100 for 15 min. To block nonspecific antibody binding, 10% boiled donkey serum (BDS) was added to the cells and left to incubate for 60 min at room temperature. Antibodies were prepared in 5% BDS and used at the following concentrations: Hec1 (9G3) at 1:1000 (GeneTex, Irvine, CA), ACA (anti-centromere antibody) at 1:300 (Antibodies Inc., Davis, CA), α-tubulin at 1:200 (Sigma, St. Louis, MO), α-Ska1 at 1:3000, α-Rama1 at 1:3000, α-KNL1 at 1:500 (Ska1, Rama1, and KNL1 antibodies were generous gifts from Iain Cheeseman), α-CLASP1 at 1:1000 (a generous gift from Helder Maiato), α-ZW10 at 1:500 (Abcam, Boston, MA), and α-CENP-E at 1:500 (Abcam). Secondary antibodies conjugated to Cy5, Alexa488, or Rhodamine RedX (Jackson ImmunoResearch, West Grove, PA) were used at a dilution of 1:300. Primary antibodies were incubated with the samples overnight at 4°C, and then coverslips were washed for 15 min in PHEM + 0.1% Triton-X 100 and rinsed with PHEM. Secondary antibodies were applied to the samples for 45 min at room temperature. Coverslips were washed for 15 min in PHEM + 0.1% Triton-X 100, counterstained with 4′,6-diamidino-2-phenylindole (DAPI; 1:50,000 in PHEM buffer), and mounted in an antifade solution containing 90% glycerol and 0.5% *N*-propyl gallate. Cells were initially chosen for analysis if they were both Cy5-positive (siRNA) and GFP-positive (Nuf2 or Hec1-GFP fusion protein). All microscopy was performed using a DeltaVision PersonalDV Imaging System (Applied Precision, Issaquah, WA) equipped with a Photometrics CoolSnap HQ2 camera (Roper Scientific, Trenton, NJ) and a 60×/1.42NA Planapochromat DIC oil immersion lens (Olympus, Center Valley, PA). For fixed cell immunofluorescence experiments, a Z-stack composed of 40 images at 0.2-µm intervals was acquired for each cell. For time-lapse microscopy Leibovitz's L-15 medium without phenol red supplemented with 10% FBS and 4.5 g/l glucose were added to live cells cultured in glass bottomed dishes (MatTek). A Precision Control WeatherStation was used throughout time-lapse imaging to maintain stage temperature at 37°C. GFP, mCherry, and DIC images were captured from a single Z plane every 4 min for up to 5 h. Kinetochore fluorescence intensities were measured using MetaMorph software (as described in Hoffman *et al.*, 2001).

ACKNOWLEDGMENTS

We thank Keith DeLuca for technical assistance and advice on experimental techniques and O'Neil Wiggan for critical reading of the manuscript. We also thank Iain Cheeseman, Claire Walczak, Helder Maiato, and Lynne Cassimeris for sharing reagents. This work was supported by the NIH (GM088371 and K01CA125051 to JGD), the Cancer League of Colorado (fellowship to LJRS), the March of Dimes, and the Pew Scholars Program in the Biomedical Sciences.

REFERENCES

Alushin GM, Ramey VH, Pasqualato S, Ball DA, Grigorieff N, Musacchio A, Nogales E (2010). The Ndc80 kinetochore complex forms oligomeric arrays along microtubules. Nature 467, 805–810.

Biggins S, Murray AW (2001). The budding yeast protein kinase Ipl1/Aurora allows the absence of tension to activate the spindle checkpoint. Genes Dev 15, 3118–3129.

Cheeseman IM, Chappie JS, Wilson-Kubalek EM, Desai A (2006). The conserved KMN network constitutes the core microtubule-binding site of the kinetochore. Cell 127, 983–997.

Cheeseman IM, Hori T, Fukagawa T, Desai A (2008). KNL1 and the CENP-H/I/K complex coordinately direct kinetochore assembly in vertebrates. Mol Biol Cell 19, 587–594.

Ciferri C *et al*. (2008). Implications for kinetochore-microtubule attachment from the structure of an engineered NDC80 complex. Cell 133, 427–439.

Cimini D, Wan X, Hirel CB, Salmon ED (2006). Aurora kinase promotes turnover of kinetochore microtubules to reduce chromosome segregation errors. Curr Biol 16, 1711–1718.

Daum JR, Wren JD, Daniel JJ, Sivakumar S, McAvoy JN, Potapova TA, Gorbsky GJ (2009). Ska3 is required for spindle checkpoint silencing and the maintenance of chromosome cohesion in mitosis. Curr Biol 19, 1467–1472.

DeLuca JG, Gall WE, Ciferri C, Cimini D, Musacchio A, Salmon ED (2006). Kinetochore microtubule dynamics and attachment stability are regulated by Hec1. Cell 127, 969–982.

DeLuca JG, Howell BJ, Canman JC, Hickey JM, Fang G, Salmon ED (2003). Nuf2 and Hec1 are required for retention of the checkpoint proteins Mad1 and Mad2 to kinetochores. Curr Biol 13, 2103–2109.

DeLuca JG, Moree B, Hickey JM, Kilmartin JV, Salmon ED (2002). hNuf2 inhibition blocks stable kinetochore-microtubule attachment and induces mitotic cell death in HeLa cells. J Cell Biol 159, 549–555.

Ditchfield C, Johnson VL, Tighe A, Ellston R, Haworth C, Johnson T, Mortlock A, Keen N, Taylor SS (2003). Aurora B couples chromosome alignment with anaphase by targeting BubR1, Mad2, and Cenp-E to kinetochores. J Cell Biol 161, 267–280.

Dougherty GW, Adler HJ, Rzadzinska A, Gimona M, Tomita Y, Lattig MC, Merritt RC Jr, Kachar B (2005). CLAMP, a novel microtubule-associated protein with EB-type calponin homology. Cell Motil Cytoskeleton 62, 141–156.

Gaitanos TN, Santamaria A, Jeyaprakash AA, Wang B, Conti E, Nigg EA (2009). Stable kinetochore-microtubule interactions depend on the Ska complex and its new component Ska3/C13Orf3. EMBO J 10, 1442–1452.

Gimona M, Djinovic-Carugo K, Kranewitter WJ, Winder SJ (2002). Functional plasticity of CH domains. FEBS Lett 1, 98–106.

Guimaraes G, Dong Y, McEwen BF, DeLuca JG (2008). Kinetochore-microtubule attachment relies on the disordered N-terminal tail domain of Hec1. Curr Biol 18, 1778–1784.

Hanisch A, Silljé HH, Nigg EA (2006). Timely anaphase onset requires a novel spindle and kinetochore complex comprising Ska1 and Ska2. EMBO J 23, 5504–5515.

Hauf S, Cole RW, LaTerra S, Zimmer C, Schnapp G, Walter R, Heckel A, van Meel J, Rieder CL, Peters JM (2003). The small molecule Hesperadin reveals a role for Aurora B in correcting kinetochore-microtubule attachment and in maintaining the spindle assembly checkpoint. J Cell Biol 161, 281–294.

Hayashi I, Ikura M (2003). Crystal structure of the amino-terminal microtubule-binding domain of end-binding protein 1 (EB1). J Biol Chem 38, 36430–36434.

Hoffman DB, Pearson CG, Yen TJ, Howell BJ, Salmon ED (2001). Microtubule-dependent changes in assembly of microtubule motor proteins and mitotic spindle checkpoint proteins at PtK1 kinetochores. Mol Biol Cell 12, 1995–2009.

Hori T, Haraguchi T, Hiraoka Y, Kimura H, Fukagawa T (2003). Dynamic behavior of Nuf2-Hec1 complex that localizes to the centrosome and centromere and is essential for mitotic progression in vertebrate cells. J Cell Sci 116, 3347–3362.

Lampson MA, Kapoor TM (2005). The human mitotic checkpoint protein BubR1 regulates chromosome-spindle attachments. Nat Cell Biol 7, 93–98.

Martin-Lluesma S, Stucke VM, Nigg EA (2002). Role of Hec1 in spindle checkpoint signaling and kinetochore recruitment of Mad1/Mad2. Science 297, 2267–2270.

McCleland ML, Kallio MJ, Barrett-Wilt GA, Kestner CA, Shabanowitz J, Hunt DF, Gorbsky GJ, Stukenberg PT (2004). The vertebrate NDC80 complex contains Spc24 and Spc25 homologs, which are required to establish and maintain kinetochore-microtubule attachment. Curr Biol 14, 131–137.

Miller SA, Johnson ML, Stukenberg PT (2008). Kinetochore attachments require an interaction between unstructured tails on microtubules and Ndc80(Hec1). Curr Biol 18, 1785–1791.

Pinsky BA, Kung C, Shokat KM, Biggins S (2006). The Ipl1-Aurora protein kinase activates the spindle checkpoint by creating unattached kinetochores. Nat Cell Biol 8, 78–83.

Powers AF, Franck AD, Gestaut DR, Cooper J, Gracyzk B, Wei RR, Wordeman L, Davis TN, Asbury CL (2009). The Ndc80 kinetochore complex forms load-bearing attachments to dynamic microtubule tips via biased diffusion. Cell 5, 865–875.

Raaijmakers JA, Tanenbaum ME, Maia AF, Medema RH (2009). RAMA1 is a novel kinetochore protein involved in kinetochore-microtubule attachment. J Cell Sci 122, 2436–2445.

Slep KC, Vale RD (2007). Structural basis of microtubule plus end tracking by XMAP215, CLIP-170, and EB1. Mol Cell 6, 976–991.

Tanaka TU, Rachidi N, Janke C, Pereira G, Galova M, Schiebel E, Stark MJ, Nasmyth K (2002). Evidence that the Ipl1-Sli15 (Aurora kinase-INCENP) complex promotes chromosome biorientation by altering kinetochore-spindle pole connections. Cell 108, 317–329.

Theis M *et al*. (2009). Comparative profiling identifies C13orf3 as a component of the Ska complex required for mammalian cell division. EMBO J 28, 1453–1465.

Wan X *et al*. (2009). Protein architecture of the human kinetochore microtubule attachment site. Cell 137, 672–684.

Wei RR, Al-Bassam J, Harrison SC (2007). The Ndc80/HEC1 complex is a contact point for kinetochore-microtubule attachment. Nat Struct Mol Biol 14, 54–59.

Welburn JP, Grishchuk EL, Backer CB, Wilson-Kubalek EM, Yates JR 3rd, Cheeseman IM (2009). The human kinetochore Ska1 complex facilitates microtubule depolymerization-coupled motility. Dev Cell 16, 374–385.

Welburn JP, Vleugel M, Liu D, Yates JR 3rd, Lampson MA, Fukagawa T, Cheeseman IM (2010). Aurora B phosphorylates spatially distinct targets to differentially regulate the kinetochore-microtubule interface. Mol Cell 38, 383–392.

Wigge PA, Kilmartin JV (2001). The Ndc80p complex from Saccharomyces cerevisiae contains conserved centromere components and has a function in chromosome segregation. J Cell Biol 152, 349–360.

Wilson-Kubalek EM, Cheeseman IM, Yoshioka C, Desai A, Milligan RA (2008). Orientation and structure of the NDC80 complex on the microtubule lattice. J Cell Biol 6, 1055–1061.